Accelerated ocean acidification in the Tsugaru Strait by an intensified Tsugaru Warm Current

M. Wakita[1], K. Sasaki[1], A. Nagano[2], H. Abe[1, 3], T. Tanaka[4], K. Nagano[5], K. Sugie[2], K. Kimoto[2], T. Okunishi[4], M. Takada[6], J. Yoshino[6], and S. Watanabe[1]

[1]Mutsu Institute for Oceanography, Research Institute for Global Change, Japan Agency for Marine-Earth Science and Technology, Mutsu, Japan.

[2]Research Institute for Global Change, Japan Agency for Marine-Earth Science and Technology, Yokosuka, Japan.

[3]Faculty of Fisheries Sciences, Hokkaido University, Hakodate, Japan.

[4]Fisheries Resources Institute, Japan Fisheries Research and Education Agency, Shiogama, Japan.

[5]Fisheries Research Institute, Aomori Prefectural Industrial Technology Research Center, Aomori, Japan.

[6]Tohoku Environmental Science Services Corporation, Rokkasho, Japan.

Corresponding author: Masahide Wakita (mwakita@jamstec.go.jp)

Key Points

- Acidification in the eastern part of the Tsugaru Strait is found to have advanced considerably throughout its depth during 2012–2019
- Acidification is occurring at faster rates than reported elsewhere and faster than expected for oceanic uptake of anthropogenic CO_2
- The accelerated acidification is caused by enhanced increase of dissolved inorganic carbon, owing to a strengthened Tsugaru Warm Current

Abstract

The oceanic uptake of anthropogenic CO_2 has resulted in acidification in surface and subsurface waters throughout the global ocean. We initiated acidification monitoring in the eastern part of the Tsugaru Strait, which connects the Sea of Japan and the North Pacific. Annual mean pH and $CaCO_3$ saturation state decreased considerably throughout all depths at rates of 0.0030−0.0051 yr^{-1} and 0.017−0.036 yr^{-1} during 2012–2019, respectively. These rates of decrease are faster than those caused by increasing atmospheric CO_2, and faster than those observed during previous research in the Sea of Japan and the North Pacific. The accelerated acidification is attributed to enhanced increase in dissolved inorganic carbon caused by elevated mixing of the upper and deeper waters from the Sea of Japan at the western part of the strait by the strengthening of the Tsugaru Warm Current.

Plain Language Summary

Approximately 30% of the total amount of CO_2 released to the atmosphere by human activities has accumulated in the global ocean. This oceanic uptake of CO_2 has resulted in ocean acidification. In coastal waters the acidification affects marine calcifying organisms, thus coastal ecosystems may be more vulnerable to acidification than the open ocean. To examine the extent to which acidification has advanced in the eastern part of the Tsugaru Strait, which connects the Sea of Japan and the North Pacific, we initiated a time-series observation of acidification. Acidification is found to have advanced considerably across the whole depth during 2012-2019 at a rate faster than that caused by increasing atmospheric CO_2, and at the highest rates observed during previous research in the North Pacific Ocean and the Sea of Japan. The rapid acidification is found to be attributable to the enhanced rate of increase of dissolved inorganic carbon caused

by elevated mixing of the upper and deeper waters from the Sea of Japan at the western part of the strait by the strengthening of the Tsugaru Warm Current. In other straits that are connected to the open ocean, the strengthening of their throughflow may also accelerate acidification.

1 Introduction

Ocean absorption of the CO_2 released to the atmosphere by human activities (i.e., anthropogenic CO_2) results in acidification of surface waters as the result of the increase in hydrogen ion (H^+) concentration. The oceanic uptake of anthropogenic CO_2 has decreased ocean pH by 0.1 since the beginning of the industrial era (Intergovernmental Panel on Climate Change, 2013). Ocean acidification also lowers the $CaCO_3$ saturation state (Ω) by decreasing carbonate ion (CO_3^{2-}) concentration with concomitant formation of bicarbonate ions. The carbonate chemistry change affects marine calcifying organisms with carbonate shells and skeletons, biogeochemical cycling of nutrients, and ecosystems (e.g., Doney et al., 2009; Sugie et al., 2018).

In the open ocean, the acidification of surface water has been well documented with time-series data at CO_2 monitoring sites (e.g., Astor et al., 2013; Bates et al., 2012; Currie et al., 2011; Dore et al., 2009; González-Dávila et al., 2010; Olafsson et al., 2010; Ono et al., 2019; Wakita et al., 2017). The rates Olausson of decrease in surface water pH are mostly within the range of 0.0013–0.0024 yr^{-1}, as expected from the response to the release of anthropogenic CO_2. Furthermore, in coastal waters, acidification affects marine calcifying organisms; for example, causing mass death of oyster larvae (e.g., Feely et al., 2008) and damage to the carapaces of larval Dungeness crabs (Bednaršek et al., 2020) along the continental shelf from central Canada to northern Mexico. The serious threats that coastal calcifying organisms have already faced suggest that coastal ecosystems may be more vulnerable to ocean acidification than the open ocean.

Japanese coastal waters are also acidified by the oceanic uptake of increased anthropogenic CO_2 in the atmosphere (Chen et al., 2017; Ishii et al., 2011; Ishizu et al., 2019;

Lui & Chen, 2015). In this study, we focus on the acidification of coastal water at the Tsugaru Strait. The strait is 100 km in length, 20–40 km in width, and has shallow sills (~130 m depth) near its western part (Figure 1). The Tsugaru Warm Current (TWC) flows eastward from the Sea of Japan into the North Pacific (annual mean volume transport 1.5 Sv; 1 Sv = 10^6 m^3 s^{-1}) and is driven principally by sea level difference between the Sea of Japan and the North Pacific (e.g., Ito et al., 2003; Toba et al., 1982). Primary productivity and nutrients increase downstream along the TWC (Matsuura et al., 2007; Saitoh et al., 2008; Yamada et al., 2005) and fishery resources (e.g., scallop, abalone, sea urchin, squid, and Pacific bluefin tuna) are abundant (e.g., Kosaka, 2016; Sakurai et al., 2000; Shimose & Ishihara 2015). Recently, Ohta et al. (2015) revealed vigorous vertical turbulent mixing over the abrupt bottom of the sills in the western part of the Tsugaru Strait. Vertical turbulent flows mix the warm fresh upper water in the Tsugaru Strait with the cold saline deeper water transported by the Tsushima Warm Current in the Sea of Japan into the strait. The vigorous vertical turbulent mixing just east of the sills is thought to enhance nutrients and to maintain high productivity.

In the Sea of Japan (i.e., the upstream part of the TWC) subsurface waters at depths below 300 m are acidifying at a rapid rate (–0.002 to –0.004 yr^{-1}), owing to the increasing atmospheric CO_2 and increase in DIC associated with deoxygenation under reduced ventilation (Chen et al., 2017). The rapidly acidified water is thought to be transported into the Tsugaru Strait. Furthermore, the volume transport of the Tsushima Warm Current has increased considerably from 2005 to 2017, as observed at the eastern channel of the Tsushima Strait by ship-mounted Acoustic Doppler Current Profiler (Shibano et al., 2019). These changes in the Sea of Japan might enhance the ocean acidification in the eastern part of the Tsugaru Strait by vertical turbulent mixing in the western part.

To examine the extent to which ocean acidification has progressed at various depths in the Tsugaru Strait, we initiated a time-series observation of ocean acidification in February 2014 by measuring temperature, salinity, nutrients, dissolved inorganic carbon (DIC), and total alkalinity (TA) by weekly bucket sampling at the breakwater of Sekinehama Port (BW) of the Mutsu Institute of Oceanography, Japan Agency for Marine-Earth Science and Technology (JAMSTEC), located on the northern coast of the Shimokita Peninsula of the eastern Tsugaru Strait (Figure 1). In addition, ship-based observations in the eastern part of the strait (stations SE3, SE9, OS1 and HO3) have been performed every season since the summer of 2012.

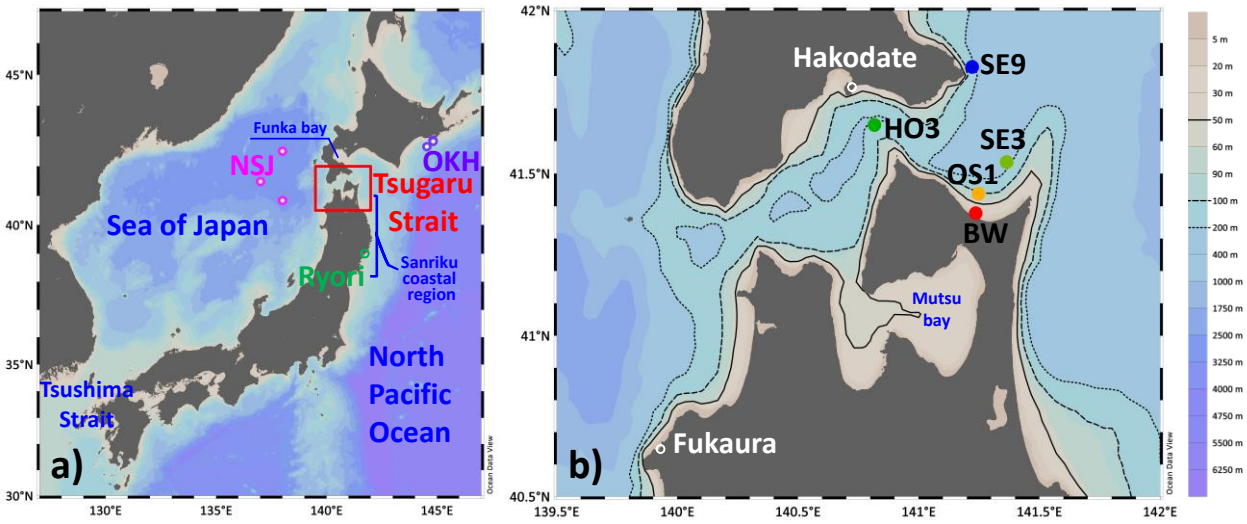

Figure 1. Maps of the observation area and location of the sampling station near the islands of Japan. In the overview map (a), NSJ and OKH indicate the stations in the northern Sea of Japan and off Kushiro at Hokkaido island, respectively. Ryori is the time-series station for atmospheric CO_2 monitoring by the Japan Meteorological Agency (green open circle). The enlarged map (b) shows the time-series stations for ocean acidification monitoring in the eastern part of Tsugaru Strait (colored circles) and sea level monitoring (white open circles). Solid, dashed, and dotted lines indicate the 50, 100, and 200 m isobaths, respectively.

2 Observations and Data

2.1 Time-series observation of ocean acidification

We performed the time-series observations at the end of the breakwater (the water depth is 9 m) in Sekinehama Port (station BW) by bucket surface water sampling and conductivity-temperature-depth (CTD; RINKO-Profiler; JFE Advantech Co., Ltd.) measurements every week from February 2014 to December 2019 (Wakita, 2020). In this study, we used samples collected from 325 bucket casts at station BW.

The CTD SBE 911plus (Sea-Bird Scientific , Inc.) observations and water sampling with bucket and Niskin bottle were performed from the sea surface to the seafloor at stations SE3, SE9, OS1, and HO3 every season during 2010−2019 onboard Japanese training ships (*Ushio-Maru* and *Oshoro-Maru* of Hokkaido University: spring 2010 to fall 2019) and research vessels (*Wakataka-Maru* of the Japan Fisheries Research and Education Agency: summer 2018 and 2019, *Kaiun-Maru* of the Aomori Prefectural Industrial Technology Research Center: winter 2019). We started to collect water samples for DIC and TA from summer 2012. We used a total of 103 CTD casts in 35 cruises at stations SE3, SE9, OS1 and HO3.

As reference water properties for the water masses flowing into the Tsugaru Strait, we used physical and biogeochemical data from station NSJ (Sea of Japan Water) in the northern part of the Sea of Japan in 2013 (KS13-08) acquired by the R/V *Keifu-Maru* of the Japan Meteorological Agency (JMA) and station OKH (Coastal Oyashio Water) off Kushiro at Hokkaido island in 2015 (KH-15-1) acquired the JAMSTEC R/V *Hakuho-Maru*.

We used coulometric and potentiometric techniques to measure DIC with coulometers (CM5012, UIC, Inc; MODEL 3000A, Nippon ANS, Inc.) and TA using a total alkalinity titration analyzer (ATT-05, Kimoto Electric Co., Ltd.) (Wakita et al., 2017). The values were calibrated against certified reference material provided by Prof. A. G. Dickson (Scripps Institution of Oceanography, University of California San Diego) and reference material produced by KANSO Co., Ltd. The precision of the analyses for both the DIC and TA measurements was within ±0.8 μmol kg^{-1}, based on replicate samples. The values of nutrients (silicate, SiO_2, and phosphate, PO_4) and salinity were measured with a continuous flow analyzer (QuAAtro, BL TEC K.K.) and a salinometer (Model 8400B AUTOSAL, Guildline Instruments Ltd.), respectively. These values were calibrated against certified reference material provided by KANSO Co., Ltd (for nutrients) and IAPSO Standard Seawater provided by Ocean Scientific International Ltd (for salinity). Based on replicate samples, the precisions for SiO_2, PO_4 and salinity were within ±0.2 μmol kg^{-1}, ±0.01 μmol kg^{-1}, and ±0.001, respectively. The values of DIC, TA, SiO_2, and PO_4 were normalized to a salinity of 35.0 to correct for the dilution and concentration of seawater by evaporation and precipitation and are expressed here as nDIC, nTA $nSiO_2$ and nPO_4, respectively (e.g., nDIC = DIC × 35/salinity).

We used the CO2SYS program developed by Lewis and Wallace (1998) with the carbonate dissociation constants of Mehrbach et al. (1973) refitted by Dickson and Millero (1987), and values for temperature, salinity, DIC, TA, SiO_2, and PO_4 to calculate the pH (in total hydrogen ion concentration scale) at the in situ temperature and 25°C ($pH_T^{\text{in situ}}$ and pH_T^{25}) and Ω (Ω = $[Ca^{2+}][CO_3^{2-}]\cdot K_{sp}^{-1}$ where K_{sp} is the apparent solubility product of calcite or aragonite; Mucci, 1983). Values of Ω were calculated with respect to the mineral forms of $CaCO_3$,

aragonite ($\Omega_{aragonite}$). We estimated [Ca^{2+}] by assuming that [Ca^{2+}] was directly proportional to salinity (Millero, 1982).

2.2 Tide gauge data

The TWC is driven principally by sea level difference across the Tsugaru Strait (e.g., Toba et al., 1982). Hourly sea level data are collected by the JMA at two coastal tide gauge stations, Fukaura and Hakodate (Figure 1b). Because the sea level difference between Fukaura and Hakodate is well correlated to the volume transport of the TWC, the sea level difference has been used as an indicator of volume transport of the TWC (e.g. Nishida et al., 2003). To correct the influence of vertical crustal movement, changes of the local reference levels observed on the first day of each year by the JMA (https://www.data.jma.go.jp/kaiyou/db/tide/suisan/station.php) were interpolated linearly at 1 hour intervals and subtracted from the hourly sea level at each station. In addition, the baselines of the tide gauge stations have been converted from the local reference levels to the mean sea level of Tokyo Bay. Further, tidal variations were suppressed by a tide-eliminating filter of Thompson (1983). After averaging to obtain daily data, atmospheric pressure correction was conducted using the daily mean sea level pressure observed at each tide gauge station. We used the daily mean sea level difference of Fukaura minus Hakodate.

2.3 Calculation of deseasonalized annual mean values

At the Tsugaru Strait, there are substantial seasonal variations in current velocity and water properties (e.g. Matsuura et al., 2007; Saitoh et al., 2008), which may yield a seasonal bias in the sampling and complicate the statistical trend analysis of time-series data (Bates et al.,

2014). Physical and biogeochemical data obtained by bucket surface water sampling are in agreement with those at 10 m depth from Niskin bottle water sampling (not shown). For the surface water down to 10 m depth, following Takahashi et al. (2006), we calculated mean values of the physical and chemical parameters for every month to obtain mean seasonal variations. For subsurface waters (below 20 m depth), we calculated mean values of the parameters for every season (winter from January to March, spring from April to June, summer from July to September, and fall from October to December) as in Bates et al. (2014), because the number of subsurface samples (103) is not sufficient to obtain significant mean values for each month.

For example, the deseasonalized monthly (seasonal) mean value of nDIC, $nDIC_{deseasonalized}$, in the surface (subsurface) water was calculated as follows:

$$nDIC_{deseasonalized} = nDIC_{obs}^{\text{month or season}} - nDIC_{mean}^{\text{month or season}} + nDIC_{mean}^{\text{annual}}$$

where $nDIC_{obs}^{\text{month or season}}$ is the observed value of nDIC during a month for the surface water, or a season for the subsurface water. $nDIC_{mean}^{\text{month or season}}$ is the surface monthly or subsurface seasonal mean value of nDIC, and sufficient $nDIC_{mean}^{\text{annual}}$ is the annual mean value. The rates of change of these deseasonalized monthly and seasonal mean time series were calculated using a linear least-squares method.

3 Results and Discussion

3.1 Hydrographic features in the eastern part of the Tsugaru Strait

At stations HO3, SE3 and OS1 in the eastern part of the strait, temperature, salinity, nDIC, nTA, and nutrients of the surface water have similar seasonal variations (Figure 2) because these stations were located in the surface water transported by the TWC throughout the year. However, the observed values during winter and spring at station SE9 are similar to those of the coastal Oyashio water (COW) at station OKH off Kushiro during the winter of 2015 (purple circles in Figure 2). This similarity between the surface water properties at SE9 and OKH indicates that the surface COW was advected from the eastern coast of Hokkaido to the northern part of the Tsugaru Strait (e.g., Saitoh et al., 2008; Shimizu et al., 2001). Notably, values of the parameters observed at station BW in Sekinehama Port agree well with those at HO3, SE3, and OS1. In other words, the surface water obtained by bucket sampling at station BW has the characteristics of surface water of the TWC, except for during the period of COW advection from January to April in 2014 (purple hatches; Figure 2).

The seasonal variations of subsurface water properties at HO3, SE3 and OS1 are similar but differ from those at SE9 (Figure S1). The amplitudes of the seasonal variations decrease with depth. The advection of the COW from February to April in 2014 (purple hatches; Figure S1) extended to a depth of 20 m, as salinity, nTA and nDIC at SE9, SE3, OS1, and HO3 are similar to COW (purple circles). However, in this period, the water below 50 m depth at SE3, OS1, and HO3 was occupied by northern Sea of Japan water (SJW), as observed at station NSJ in the fall of 2013 (pink circles). Therefore, the eastern part of the Tsugaru Strait (stations HO3, SE3, OS, and BW) was dominated by TWC water through all depth layers from 2012 to 2019, except from during February to May in 2014 when it was affected by the COW and the northern SJW. In this study, we analyzed data at stations HO3, SE3, OS1, and BW to examine the temporal changes of TWC water after excluding the data collected during February to May in 2014.

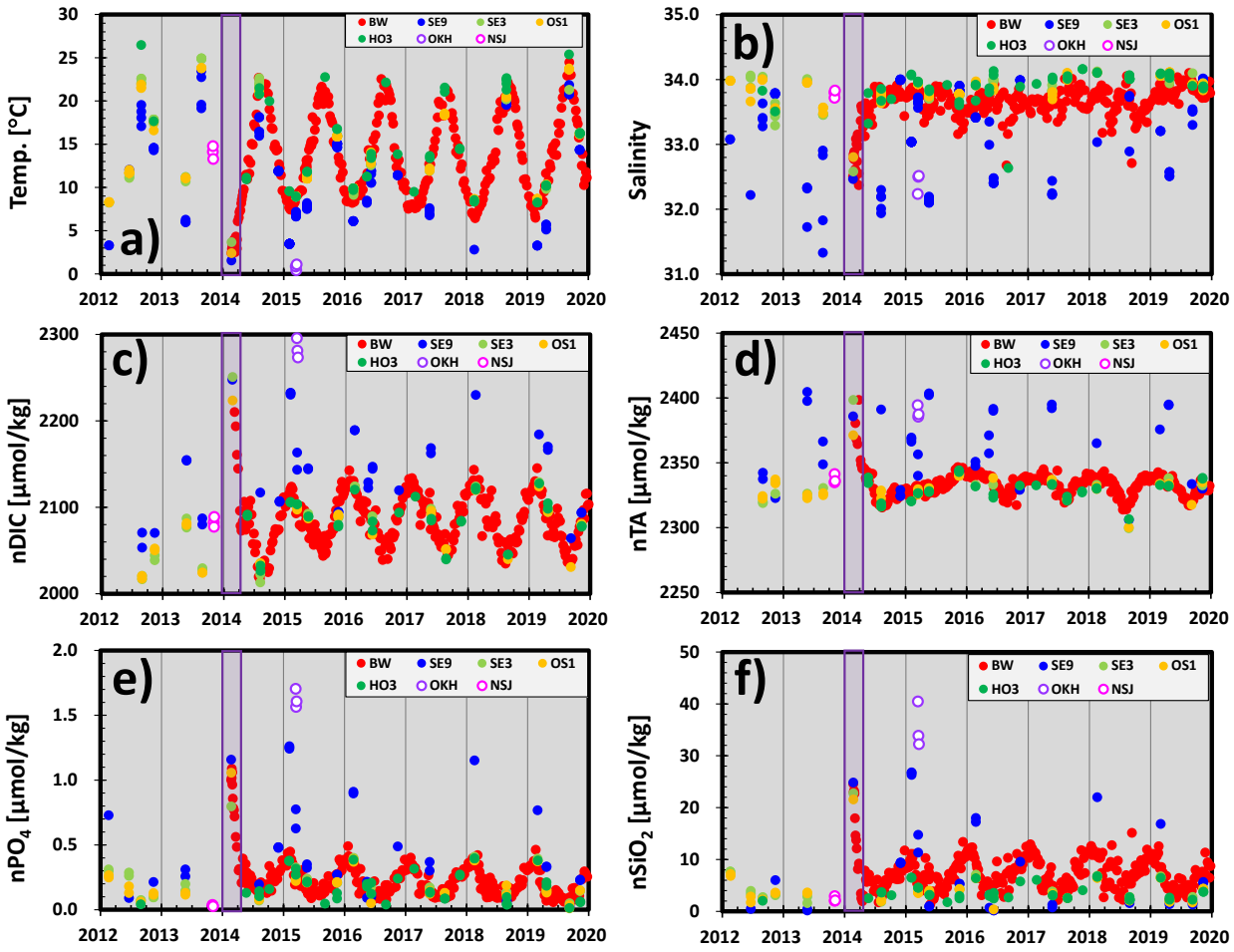

Figure 2. Time-series of (a) temperature, (b) salinity, (c) nDIC, (d) nTA, (e) nPO_4, and (f) $nSiO_2$ in the surface water (0–10 m depth) in the eastern part of the Tsugaru Strait, in the northern part of the Sea of Japan, and in the region off Kushiro, Hokkaido Island. Colors of plotted circles are the same as those of the sampling stations shown in Figure 1. The period of the COW intrusion from January to April in 2014 is indicated by purple hatches.

3.2 Accelerated acidification of the TWC water

During 2012−2019, the deseasonalized annual mean values of $pH_T^{in\ situ}$, $\Omega_{aragonite}$, and nDIC in the surface water and subsurface water changed considerably at rates of −0.0030 to −0.0051 yr^{-1} ($p < 0.05$), −0.017 to −0.036 /yr^{-1} ($p < 0.05$), and 1.9 to 3.6 µmol kg^{-1} yr^{-1} ($p < 0.05$), respectively (Figures 3 and 4), whereas nTA remained almost constant (Figures 2 and S1). These rates in the surface water ($pH_T^{in\ situ}$: −0.0030 ± 0.0005 yr^{-1}; $\Omega_{aragonite}$: −0.017 ± 0.003 yr^{-1} and nDIC: 1.9 ± 0.3 µmol kg^{-1} yr^{-1}) were higher than those at time-series sites in other open oceans ($pH_T^{in\ situ}$: −0.0014 to −0.0026 yr^{-1}; $\Omega_{aragonite}$: −0.002 to –0.012 yr^{-1} and nDIC: 0.8 to 1.9 µmol kg^{-1} yr^{-1}) summarized by Bates et al. (2014), and those predicted from oceanic equilibration with the increasing atmospheric CO_2 (2.4 µatm yr^{-1}) at station Ryori (Figure 1a) from 2012 to 2019 ($pH_T^{in\ situ}$: −0.0022 yr^{-1}; $\Omega_{aragonite}$: −0.0012 yr^{-1} and nDIC: 1.4 µmol kg^{-1} yr^{-1}) (Figure 4). The $pH_T^{in\ situ}$ decline of the surface water is faster than that of the other coastal waters around Japan ($pH_T^{in\ situ}$: −0.002 yr^{-1}; Chen et al., 2017; Ishii et al., 2011; Ishizu et al., 2019; Lui & Chen, 2015).

In the subsurface layers, the rates of change of pH, $\Omega_{aragonite}$ and nDIC were estimated to be −0.0043 to −0.0051 yr^{-1} ($p < 0.05$), −0.024 to −0.036 /yr^{-1} ($p < 0.05$), and 2.8 to 3.6 µmol kg^{-1} yr^{-1} ($p < 0.05$), respectively (Figure 4). These rates are higher than for the surface water. This $pH_T^{in\ situ}$ decline was faster than the highest rates (−0.004 yr^{-1}) in the North Pacific at 200−500 m depth between 1991 and 2006 (Byrne et al., 2010) and in the Sea of Japan at 300 m depth between 1965 and 2015 (Chen et al., 2017). Evidently, the progress of acidification of the TWC water is rapid across all depths, particularly in the subsurface layer, compared with the surrounding oceans.

To identify the factors that account for the accelerated acidification, we examined the water properties that mainly control the rapid trends in $pH_T^{\text{in situ}}$ and $\Omega_{\text{aragonite}}$. Note that $pH_T^{\text{in situ}}$ and $\Omega_{\text{aragonite}}$ are functions of the pressure, temperature, salinity, DIC, TA, phosphate, and silicate of the TWC water. Following Wakita et al. (2013), we evaluated the trends in pH_T by allowing one parameter to vary while fixing the other parameters to the mean values. For example, we estimated the contribution of the nDIC or temperature to the decline of pH_T at 100 m depth by calculating the pH change using nDIC or temperature and mean values for the other parameters. The decline of $pH_T^{\text{in situ}}$ (-0.0043 yr^{-1}) at 100 m depth is enhanced by nDIC (-0.0065 yr^{-1}) and is suppressed by temperature ($+0.0022$ yr^{-1}), because temperature in TWC during 2012−2019 did not increase significantly, despite global warming (not shown). The $pH_T^{\text{in situ}}$ decline between 20 m and 50 m (-0.0043 to -0.0051 yr^{-1}) were slower than pH_T^{25} (-0.0058 to -0.0075 yr^{-1}; Figure 4). Namely, the temperature variation mitigates the pH_T decline. Thus, the increases in nDIC (1.9 to 3.6 μmol kg^{-1} yr^{-1}) are the main driver of the accelerated acidification, and are significantly higher than those due to the increasing atmospheric CO_2 (1.4 to 2.0 μmol kg^{-1} yr^{-1}; Figure 4). The rapid acidification is attributed to the enhanced rate of increase of nDIC caused by the oceanic uptake of anthropogenic CO_2 and other physical and/or biogeochemical processes.

In addition to the trends of water properties, the volume transport of the TWC changed considerably during the study period. The sea level difference between Fukaura and Hakodate, a TWC transport index (e.g., Nishida et al., 2003), increased significantly at a rate of 0.26 ± 0.03 cm yr^{-1} ($p < 0.001$) during 2010−2019 (Figure 3f), consistent with the increase in volume transport of the Tsushima Warm Current reported by Shibano et al. (2019).

The intensification of the TWC is thought to increase the inflow to the Tsugaru Strait of deep water with high DIC associated with deoxygenation due to organic matter decomposition

283 under reduced ventilation in the Sea of Japan (Chen et al., 2017). This deeper water (saline, cold,
284 high DIC) is possibly mixed into the upper layer via enhanced vertical turbulent mixing in the
285 western part of the Tsugaru Strait,

286 hich is consistent with our observations of a significant increase in salinity, but not
287 temperature, in the eastern part of the Tsugaru Strait (Figure 3e).

288 We discuss the impact of enhanced mixing of the deep high-DIC water in the Sea of
289 Japan on the increase in nDIC in the eastern part of the Tsugaru Strait. Due to the significant
290 salinity increase in the eastern part of the Tsugaru Strait, the potential density increased
291 considerably (Figure 3d). The potential density is found to be linearly related to the nDIC
292 increase (Figure S2). We use the linear relationship between potential density and nDIC to
293 evaluate the impact of the increase of potential density water via enhanced mixing in the increase
294 of nDIC. The slope of the Deming linear regression line (Deming, 1943) between nDIC and
295 potential density is 26.7 ± 0.5 μmol m^3 kg^{-2} (r = 0.89, p < 0.0001). Based on the regression, we
296 calculated the rate of increase of nDIC due to the potential density increase (0.019 to 0.046 m^3
297 kg^{-1} yr^{-1}) to be 0.5 to 1.2 μmol kg^{-1} yr^{-1}. The increase in nDIC expected from oceanic
298 equilibration with increasing atmospheric CO_2 is 1.4 to 2.0 μmol kg^{-1} yr^{-1}. The sum of the two
299 components is 1.9 to 3.0 μmol kg^{-1} yr^{-1}, which is in good agreement with the observed nDIC
300 increases (1.9 to 3.6 μmol kg^{-1} yr^{-1}; Figure 4). Thus, the enhanced mixing of deep high-DIC
301 water caused by the intensification of the TWC together with the absorption of atmospheric CO_2
302 are responsible for the enhancement of the increase in nDIC.

303 At 200 m depth, however, the calculated rate of nDIC increase (1.9 ± 0.8 μmol kg^{-1} yr^{-1})
304 was slightly smaller than the observed rate (2.8 ± 1.3 μmol kg^{-1} yr^{-1}). Because this occurred
305 below the abrupt sill in the western part of the Tsugaru Strait (~130 m depth), the slightly smaller

306 increase rate of nDIC at 200 m depth might be caused by the downscaling of the enhanced
307 mixing of deep high-DIC water or other processes, as there is no significant increases in salinity
308 or potential density increase ($p < 0.1$).
309

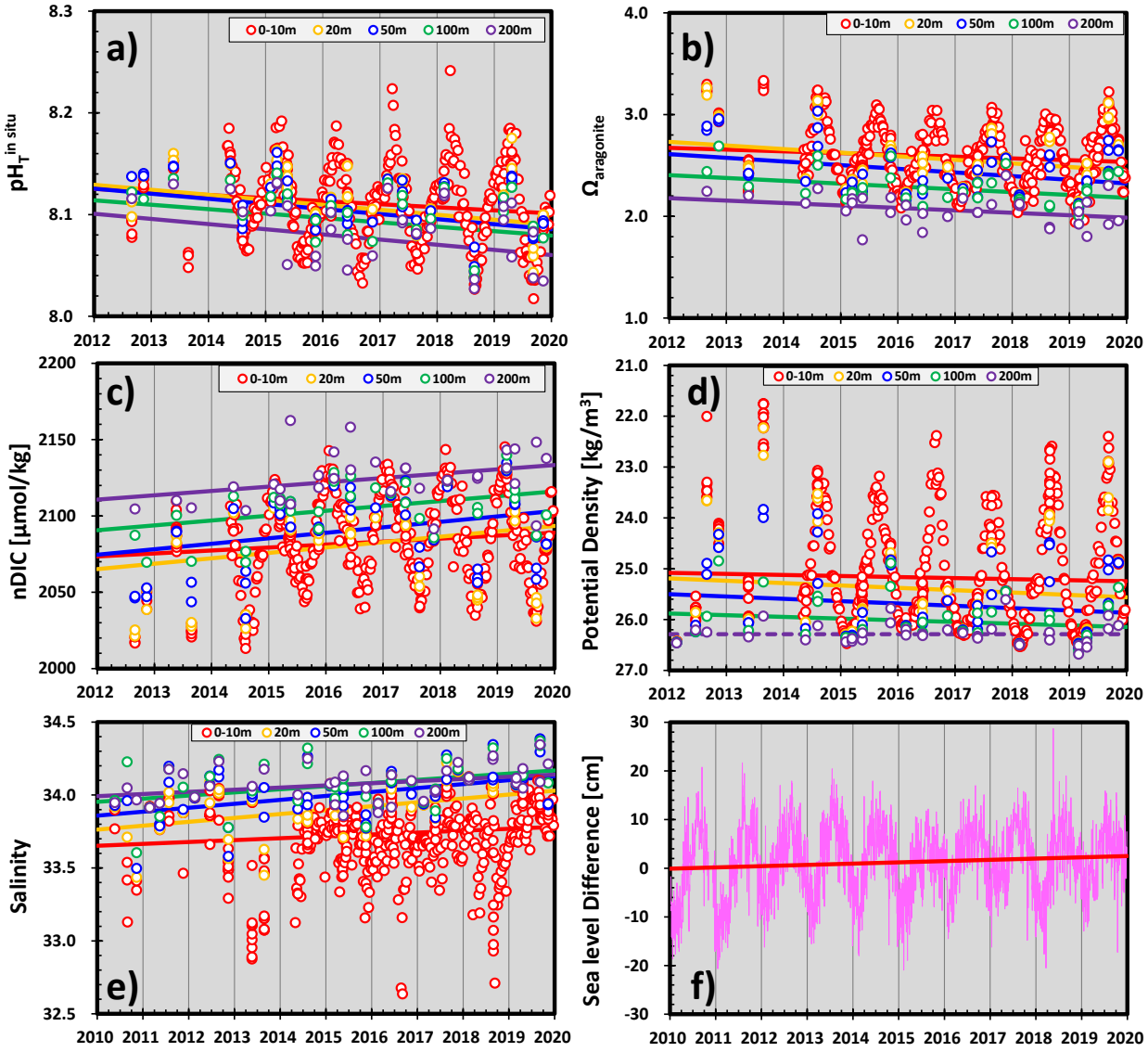

Figure 3. Time-series of (a) $pH_T^{in\ situ}$, (b) $\Omega_{aragonite}$, (c) nDIC, (d) potential density, and (e) salinity in surface water (0–10 m depth, red circles) and subsurface (20 m depth, yellow circles; 50 m depth, blue circles; 100 m depth, green circles; and 200 m depth, purple circles) water in the eastern part of the Tsugaru Strait, and (f) sea level difference (pink curve) between Fukaura and Hakodate (white circles in Figure 1). Solid (dashed) lines indicate statistically significant (insignificant) regressions ($p < 0.05$).

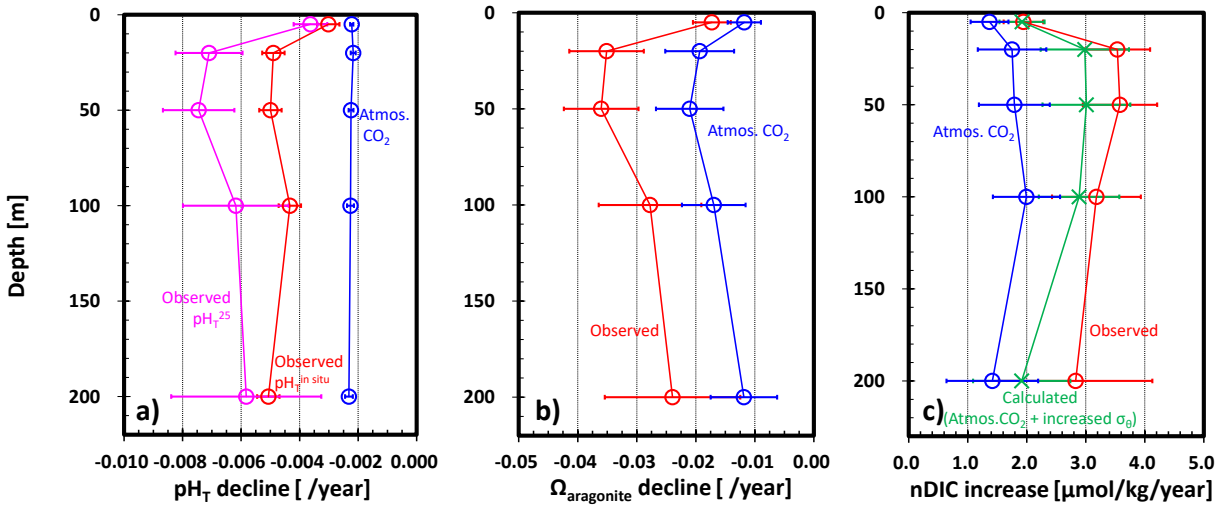

Figure 4. Rates of temporal changes in (a) pH_T, (b) $\Omega_{aragonite}$, and (c) nDIC as function of depth during 2012−2019 in the eastern part of the Tsugaru Strait. Observed rates of $pH_T^{in\ situ}$, $\Omega_{aragonite}$, and nDIC changes are indicated by red circles; predicted rates from the increasing atmospheric CO_2 at a rate of 2.4 ppm yr^{-1} observed at the JMA Ryori atmospheric monitoring station (Figure 1a) during 2012−2019 by blue circles; the rates of pH_T^{25} decline by pink circles; and calculated rates of nDIC increase due to the potential density (σ_θ) increase and the increasing atmospheric CO_2 by green crosses. The error values represented by the horizontal lines are the standard errors for the slope of the linear regressions.

4 Conclusions

We examined the acidification of the TWC water in the eastern part of the Tsugaru Strait using time-series of physical and carbonate chemical data. Annual mean $pH_T^{in\ situ}$ and $\Omega_{aragonite}$ at 0−200 m depth in the TWC water decreased significantly at rates of 0.0030−0.0051 yr^{-1} and

335 0.017−0.036 yr^{-1} during 2012–2019, respectively. Throughout all depths, the progress of the
336 acidification at the Tsugaru Strait is found to be faster than that expected from the increasing
337 atmospheric CO_2 and at time-series ocean sites in the open ocean and Japanese coastal waters.
338 More noteworthy is the fact that the highest acidification is observed in the subsurface layer at
339 20–100 m depth, and that is occurring faster than the highest rates observed during previous
340 studies in the North Pacific Ocean and the Sea of Japan. The rapid acidification is found to be
341 attributed to the enhanced increase of nDIC caused by the elevated mixing of deep high-DIC
342 water into the upper layer by the intensification of the TWC in addition to the oceanic uptake of
343 anthropogenic CO_2.

344 The accelerated acidification observed at Tsugaru Strait may also occur under the
345 influence of the TWC water in Mutsu Bay, Funka Bay, and the Sanriku coastal region (Figure 1),
346 where there are the abundant fishery resources of calcifying organisms (e.g., scallop, abalone,
347 and sea urchin). In other straits that are connected to the open ocean (e.g., the Tsushima and
348 Soya Straits), the strengthening of their throughflow may also accelerate the acidification. At
349 similar straits around the world, continuous monitoring of acidification is required to identify its
350 progression and its effect on marine calcifying species and ecosystems.

351

352 **Acknowledgments**

353 We acknowledge the help of the staff of the Mutsu Institute for Oceanography and the Research
354 Institute for Global Change of JAMSTEC, and the captains and crews of R/Vs *Ushio-Maru*,
355 *Oshoro-Maru, Wakataka-Maru*, and *Kaiun-Maru* for their kind cooperation in sample collection
356 and hydrographic measurements during the 2010–2019 cruises. The time-series data at station
357 BW from 2014 to 2019 were downloaded from the Sekinehama Port carbon time-series data in
358 the JAMSTEC Data Catalog
359 (http://www.godac.jamstec.go.jp/catalog/data_catalog/metadataDisp/Sekinehama_carbon_data?l
360 ang=en&view=simple). Physical and biogeochemical data were obtained in 2013 (KS13-08) by
361 the JMA (http://www.data.jma.go.jp/gmd/kaiyou/db/vessel_obs/data-

report/html/ship/cruisedata_e.php?id=KS1308). Atmospheric CO_2 contents at station Ryori were observed by the JMA from 2012 to2019 (https://www.data.jma.go.jp/ghg/kanshi/ghgp/co2_e.html#distribution). During 2010−2019, the JMA measured hourly sea level data and atmospheric pressure at two coastal tide gauge stations, Fukaura and Hakodate (https://www.data.jma.go.jp/kaiyou/db/tide/genbo/index.php; https://www.data.jma.go.jp/gmd/risk/obsdl/index.php; theses data are not available in English). For their valuable comments and discussion, we thank Mr. T. Tanaka, Mr. K. Fujikura, Mrs. S. Tatamisashi, Mr. H. Yamamoto, Mr. Y. Yoshikawa, Mr. H. Kawakami, Mr. N. Harada, Mr. T. Kawano (JAMSTEC), Mr. S. Sato, Mr. Y. Kosaka, Mr. Y. Imamura, Mr. K. Noro (Aomori Prefectural Industrial Technology Research Center), Mr. K. Tsubata, Mr. T. Nishimura, Mr. T. Ohmura (Tohoku Environmental Science Services Corporation), Mr. A. Kasai, Mr. T. Hirawake, Mr. T. Isada, Mr. M. Fujii, Mr. J. Nishioka, Mr. H. Munehara (Hokkaido University), Mr. Y. Tanaka (Hachinohe Institute of Technology) and Mr. T. Ono (Japan Fisheries Research and Education Agency). We also thank the marine technicians of Marine Works Japan, Ltd. onboard R/Vs *Ushio-Maru* and *Oshoro-Maru*. This work was partly supported by a Grant-in-Aid for Scientific Research (15H02835, 20H04349) from the Ministry of Education, Culture, Sports, Science and Technology (MEXT) KAKENHI. Finally, we also express our deep thanks to the editor and two anonymous reviewers who provided many useful comments.

References

Astor, Y. M., Lorenzoni, L., Thunell, R., Varela, R., Muller-Karger, F., Troccoli, L., Taylor, G. T., Scranton, M. I., Tappa, E., & Rueda, D. (2013). Interannual variability in sea surface temperature and fCO_2 changes in the Cariaco Basin. *Deep Sea Research Part II, 93*, 33–43. https://doi.org/10.1016/j.dsr2.2013.01.002

Bates, N. R., Best, M. H. P., Neely, K., Garley, R., Dickson, A. G., & Johnson, R. J. (2012). Detecting anthropogenic carbon dioxide uptake and ocean acidification in the North Atlantic Ocean. *Biogeosciences, 9*, 2509–2522. https://doi.org/10.5194/bg-9-2509-2012

Bates, N.R., Astor, Y.M., Church, M.J., Currie, K., Dore, J.E., González-Dávila, M., Lorenzoni, L., Muller-Karger, F., Olafsson, J., & Santana-Casiano, J.M. (2014). A time-series view of changing ocean chemistry due to ocean uptake of anthropogenic CO_2 and ocean acidification. *Oceanography, 27*(1), 126–141, https://doi.org/10.5670/oceanog.2014.16

Bednaršek, N., Feely, R. A., Beck, M. W., Alin, S. R., Siedlecki, S. A., Calosi, P., Norton, E. L., Saenger, C., Štrusg, J., Greeley, D., Nezlin, N. P., Roethler, M., & Spicer, J. I. (2020). Exoskeleton dissolution with mechanoreceptor damage in larval Dungeness crab related to severity of present-day ocean acidification vertical gradients. *Science of The Total Environment, 716*, 136610

Byrne, R. H., Mecking, S., Feely, R. A., & Liu, X. (2010). Direct observations of basin-wide acidification of the North Pacific Ocean. *Geophysical Research Letters, 37*, L02601, https://doi.org/10.1029/2009GL040999

Chen, C. A., Lui, H.-K., Hsieh, C. H., Yanagi, T., Kosugi, N., Ishii, M., & Gong, G. C. (2017). Deep oceans may acidify faster than anticipated due to global warming. *Nature Climate Change, 7*(12), 890–894. https://doi.org/10.1038/s41558-017-0003-y

Currie, K.I., Reid, M.R., & Hunter, K.A. (2011). Interannual variability of carbon dioxide drawdown by subantarctic surface water near New Zealand. *Biogeochemistry, 104*, 23–34, https://doi.org/10.1007/s10533-009-9355-3

Dickson, A. G., & Millero, F. J. (1987). A comparison of the equilibrium-constants for the dissociation of carbonic-acid in seawater media. *Deep Sea Research Part A. Oceanographic Research Papers, 34*(10), 1733–1743, https://doi.org/10.1016/0198-0149(87)90021-5

Deming, W. E. (1943), Statistical adjustment of data. Wiley, NY.

Dore, J.E., Lukas, R., Sadler, D.W., Church, M.J., & Karl, D.M. (2009). Physical and biogeochemical modulation of ocean acidification in the central North Pacific. *Proceedings of the National Academy of Sciences, 106*, 12,235–12,240, https://doi.org/10.1073/pnas.0906044106

Doney, S. C., Fabry, V. J., Feely, R. A., & Kleypas, J. A. (2009). Ocean acidification: The other CO_2 problem. *Annual Review of Marine Science, 1*, 169–192, https://doi.org/10.1146/annurev.marine.010908.163834

Feely, R. A., Sabine, C. L., Hernandez-Ayon, J. M., Ianson, D., & Hales, B. (2008). Evidence for upwelling of corrosive "acidified" water onto the continental shelf. *Science, 320*, 1490-1492.

González-Dávila, M., Santana-Casiano, J.M., Rueda, M.J., & Llinas, O. (2010). The water column distribution of carbonate system variables at the ESTOC site from 1995 to 2004. *Biogeosciences, 7*, 3067–3081, https:// doi.org/10.5194/bg-7-3067-2010

Intergovernmental Panel on Climate Change (2013), *The Physical Science Basis. Contribution of Working Group I to the Fifth Assessment Report of the Intergovernmental Panel on Climate Change*, edited by T. F. Stocker et al., Cambridge Univ. Press, Cambridge, U. K.

Ishii, M., Kosugi, N., Sasano, D., Saito, S., Midorikawa, T., & Inoue, H. Y. (2011). Ocean acidification off the south coast of Japan: A result from time series observations of CO_2 parameters from 1994 to 2008. *Journal of Geophysical Research, 116*(C06022), https:// doi.org/10.1029/2010jc006831

Ishizu, M., Miyazawa, Y., Tsunoda, T., & Ono, T. (2019). Long-term trends in pH in Japanese coastal seawater. *Biogeosciences, 16*, 4747–4763, https://doi.org/10.5194/bg-16-4747-2019

Ito, T., Togawa, O., Ohnishi, M., Isoda, Y., Nakayama, T., Shima, S., Kuroda, H., Iwahashi, M. & Sato, C. (2003). Variation of velocity and volume transport of the Tsugaru Warm Current in the winter of 1999–2000. *Geophysical Research Letters, 30*(13), 1678, https://doi.org/10.1029/2003GL017522

Kosaka, Y. (2016). Scallop Fisheries and Aquaculture in Japan. *Developments in Aquaculture and Fisheries Science, 40*, 891–936.

Lewis, E., & Wallace, D. W. R. (1998). Program developed for CO_2 system calculations, Rep. 105, 33 pp., Oak Ridge Natl. Lab., Oak Ridge, Tenn. [Available at http://cdiac.esd.ornl.gov/oceans/co2rprt.html]

Lui, H., & Chen, C. A. (2015). Deducing acidification rates based on short-term time series. *Scientific Reports, 5*, 11517, https://doi.org/10.1038/srep11517

Matsuura, H., Isoda, Y., Kuroda, H., Kuma, K., Saitoh, Y., Kobayashi, N., Aiki, T., Wagawa, T., Yabe, I., & Hoshiba, Y. (2007). Water mass modification process of the passage- flow waters through the Tsugaru Strait. *Sky and sea, 83*, 21–35 (in Japanese with English abstract).

Mehrbach, C., Culberson, C. H., Hawley, J. E., & Pytkowicz, R. M. (1973). Measurement of the apparent dissociation constants of carbonic acid in seawater at atmospheric pressure. *Limnology and Oceanography, 18*, 897–907, https://doi.org/10.4319/lo.1973.18.6.0897

Millero, F. J. (1982). The thermodynamics of seawater. Part I. The PVT properties. *Ocean Science and Engineering, 7*, 403–460.

Mucci, A. (1983), The solubility of calcite and aragonite in sea water at various salinities, temperatures and one atmosphere total pressure. *American Journal of Science*, 238, 780–799.

Nishida, Y., Kanomata, I., Tanaka, I., Sato, S., Takahashi, S., & Matsubara, H. (2003). Seasonal and interannual variations of the volume transport through the Tsugaru Strait. *Umi no Kenkyu, 12*, 487–499 (in Japanese with English abstract).

Ohta, S., Isoda, Y., Yoshimura, S., Syouji, K., Arita, S., Kawano, K., Xiaorong, F., & Kobayashi, N. (2015). Internal tidal waves generated over the sill topography in the Tsugaru Strait. *Umi to Sora*, *90*(3), 63-84 (in Japanese with English abstract).

Olafsson, J., Olafsdottir, S.R., Benoit-Cattin, A., & Takahashi, T. (2010). The Irminger Sea and the Iceland Sea time series measurements of sea water carbon and nutrient chemistry 1983–2006. *Earth System Science Data, 2*, 99–104, https://doi.org/10.5194/essd-2-99-2010

Ono, H., Kosugi, N., Toyama, K., Tsujino, H., Kojima, A., Enyo, K, Iida, Y., Nakano, T., & Ishii, M. (2019). Acceleration of ocean acidification in the Western North Pacific. *Geophysical Research Letters*, 46, 13161–13169. https://doi.org/10.1029/2019GL085121

Saitoh, Y., Kuma, K., Isoda, Y., Kuroda, H., Matsuura, H., Wagawa, T., Takata, H., Kobayashi, N., Nagao, S., & Nakatsuka T. (2008). Processes influencing iron distribution in the coastal waters of the Tsugaru Strait, Japan. *Journal of Oceanography*, *64*, 815–830.

Sakurai, Y., Kiyofuji, H., Saitoh, S., Goto, T., & Hiyama, Y. (2000). Changes in inferred spawning areas of Todarodes pacificus (Cephalopoda: Ommastrephidae) due to changing environmental conditions. *ICES Journal of Marine Science*, *57*, 24–30.

Shibano, R., Morimoto, A., Takayama, K., Takikawa, T., & Ito, M. (2019). Response of lower trophic ecosystem in the Japan Sea to horizontal nutrient flux change through the Tsushima Strait. *Estuarine, Coastal and Shelf Science, 229*, 106386, https://doi.org/10.1016/j.ecss.2019.106386

Shimizu, M., Isoda, Y., & Baba, K. (2001). A Late Winter Hydrography in Hidaka Bay, South of Hokkaido, Japan. *Journal of Oceanography*, *57*, 385–395.

Shimose, T., & Ishihara, T. (2015). A manual for age determination of Pacific bluefin tuna Thunnus orientalis. *Bulletin of Fisheries Research Agency*, *40*, 1–11.

Sugie, K., Yoshimura, T., & Wakita, M. (2018). Impact of CO_2 on the elemental composition of particulate and dissolved organic matters of marine diatoms emerged after nutrient depletion. *Limnology and Oceanography*, 63, 1924–1943, https://doi.org/10.1002/lno.10816

Takahashi, T., Sutherland, S. C., Feely, R. A. & Wanninkhof, R. (2006). Decadal change of the surface water pCO_2 in the North Pacific: A synthesis of 35 years of observations. *Journal of Geophysical Research, 111*, C07S05, https://doi.org/10.1029/2005JC003074

Thompson, R. O. R. Y. (1983). Low-Pass Filters to Suppress Inertial and Tidal Frequencies. *Journal of Physical Oceanography*, 13, 1077–1083.

Toba, Y., Tomizawa, K., Kurasawa, Y., & Hanawa, K. (1982). Seasonal and year-to-year variability of the Tsushima-Tsugaru warm current system with its possible cause. *La mer, 20*, 41–51.

Wakita, M., (2020) Sekinehama Port carbon time-series data. JAMSTEC. https://doi.org/10.17596/0002095

Wakita, M., Nagano, A., Fujiki, T., & Watanabe, S. (2017). Slow acidification of the winter mixed layer in the subarctic western North Pacific. *Journal of Geophysical Research: Oceans, 122*, 6923–6935, https://doi.org/10.1002/2017JC013002

Wakita, M., Watanabe, S., Honda, M., Nagano, A., Kimoto, K., Matsumoto, K., Kawakami, H., Fujiki, T., Kitamura, M., Sasaki, K., Sasaoka, K., Nakano, Y., & Murata, A. (2013). Ocean acidification from 1997 to 2011 in the subarctic western North Pacific Ocean. *Biogeosciences, 10*(12), 7817–7827, https://doi.org/10.5194/bg-10-7817-2013.

Yamada, K., Ishizaka, J., & Nagata, H. (2005). Spatial and Temporal Variability of Satellite Primary Production in the Japan Sea from 1998 to 2002. *Journal of Oceanography, 61*, 857–869.